Desalination and Water Treatment
www.deswater.com

doi: 10.5004/dwt.2018.22198

111 (2018) 208–225
April

Quantum chemical and QSPR studies of bis-benzimidazole derivatives as corrosion inhibitors by using electronic and lipophilic descriptors

El Hassan El Assiri[a,*], Majid Driouch[a], Zakariae Bensouda[a], Fayssal Jhilal[a], Taoufiq Saffaj[b], Mouhcine Sfaira[a], Younes Abboud[c]

[a]*Laboratory of Materials Engineering, Modeling and Environment, LIMME, Faculty of Sciences Dhar El Mahraz, Sidi Mohamed Ben Abdellah University, USMBA, PO. Box 1796 Atlas Fez, Morocco, Tel. +212 6 74 87 08 78, email: elassirielhassan@gmail.com (El H. El Assiri), Majid.driouch.fsdm@gmail.com (M. Driouch), bensouda_zakaria@hotmail.com (Z. Bensouda), fayssaljhilal@gmail.com (F. Jhilal), msfaira@yahoo.com (M. Sfaira)*
[b]*Laboratory of Application Organic Chemistry, Faculty of Sciences and Techniques, Sidi Mohamed Ben Abdellah University, USMBA, BP 2626 route d'Immouzer-Fez, Morocco, email: saffajt@yahoo.fr (T. Saffaj)*
[c]*Laboratory of Physico-Chemistry of Applied Materials (LPCMA), Faculty of Sciences Ben M'sik, Hassan II University, Casablanca, Morocco, email: youabboud@yahoo.fr (Y. Abboud)*

Received 18 August 2017; Accepted 14 March 2018

ABSTRACT

The inhibition ability of six bis-benzimidazole derivatives against corrosion of mild steel in acidic medium was modeled by the electronic and lipophilic descriptors such as: the energy of the highest occupied molecular orbital (E_{HOMO}), the energy of the lowest unoccupied molecular orbital (E_{LUMO}), the dipole moment (μ), the molecular critical volume (V_c), the inhibitor concentration (C_i), the logarithm of the partition coefficient (log *P*), and the molecular mass (*M*), by means of quantitative structure property relationships (QSPR). To do so, the structure electronic properties of these molecules were investigated by using three quantum methods: a semi-empirical method (AM1), the Hartree-Fock method (HF) and the density functional theory method (DFT), at B3LYP/6-311G level of theory. The correlation was developed by three mathematical models, based-QSPR approaches: the multiple linear regression (MLR), the multiple polynomial regression (MPR) and the partial least squares regression (PLS). A very good determination coefficient (R^2 = 0.99), adjusted determination coefficient (R^2_{adj} = 0.99) and predicted determination coefficient (R^2_{pred} = 0.97), were obtained. The calculated inhibition efficiency increased in the order OBBI > HBBI > BBI > MBBI> BBBI > EBBI, was in good agreement with experimental results.

Keywords: Corrosion inhibition; Benzimidazole; AM1; HF; DFT (B3LYP)/6-311G; QSPR; MLR; PLS; MPR

1. Introduction

Corrosion of materials is one of the main problems in industry that is associated to significant economic losses, especially, in steel industry, where acids are being used to pickling, descaling and cleaning. Because of the high aggressiveness of the said environment, the use of inhibitors compounds containing nitrogen, oxygen and sulphur atoms such as: amines, pyridines, imidazoles and benzimidazoles represents generally, an effective means of protection against corrosion of mild steels in many industries [1–10]. The selection of an inhibitor is generally, based on its mechanism of action [11]. In fact, in the acidic media, the adsorption process of inhibitors is related to the presence of heteroatoms as well as a triple bond or an aromatic ring in their molecular structure. It requires the existence of attractive forces between the adsorbed molecule and the metal surface. According to the type of interactions, the adsorption can be physisorption, chemisorption or a combination of both. Physisorption is due to electrostatic attractive

*Corresponding author.

forces between inhibiting organic ions and the electrically charged surface of the metal. Chemisorption is due to interaction between unshared electron pairs or π-electrons of the adsorbed molecule with the metal, in order to form a coordinate type of bond [12,13]. In this context, benzimidazole and its derivatives whose basic skeleton is a bicycle containing nitrogen, are considered as a potential class of corrosion inhibitors, in hydrochloric acidic media [14–20]. They are bolaform surfactants characterized by the delocalized π-electrons in the aromatic ring and two N-hetero-atoms which facilitates their adsorption onto the metallic surface and increases their corrosion inhibition potential.

Parallel to the experimental study, several efforts are supplied, at present, to predict, in theory, the inhibiting corrosion efficiency. Indeed, the use of quantum chemical methods as a theoretical investigation is a very powerful tool, in determining the molecular characteristics to develop some insights into the corrosion inhibition mechanism [21–23]. In fact, various quantum chemical calculations have been widely used to bring about the relationship between the corrosion inhibition and the structural electronic properties of a wide range of organic corrosion inhibitors [24–27]. However, the theoretical study cannot be rigorous to report the whole experimental conditions, because of the enormous complexity of the corrosion phenomena. Then, statistical methods can supply useful qualitative and quantitative information, for a better understanding of this process.

Quantitative structure-activity relationships (QSAR) or, more general, quantitative structure-property relationships (QSPR) has proven to be versatile tools to study either chemical or biological systems. In more than 50 years of active development, the field of QSAR/QSPR modeling has grown tremendously with respect to the diversity of both methodologies and applications. In this context, several successful QSAR/QSPR models have been published over the last years which encompass a wide span of biological and physicochemical properties [28,29].

Although this approach finds broad application for assessing potential impacts of biological, chemicals, materials, and nanomaterials systems, the design of reliable statistical models usually faces multicollinearity, overfitting, and spurious variables [29,30]. To overcome these inconveniences, Todeschini and Coworkers have proposed auxiliary rules [31–33] to obtain suitable mathematical models with predictive ability, by using a minimum number of variables/descriptors. The use of this technique allows minimizing the number of variables tested, while eliminating the redundant variables or those having a negligible contribution in the model QSPR.

The choice of suitable molecules for inhibiting corrosion applications might be solved using QSPR as reported by several authors [34–39], especially, in acidic media, where the correlation has been the subject of several investigations. For instance, it has been reported by Growcock et al. [34,35], Abdul-Ahad and Al Madfai [36], Dupin et al. [38] and Lucovits et al. [38,39]. Indeed, when studying a prediction of biological activity, a large number of samples obligatory required for QSAR development. In contrast, in the field of corrosion inhibition, when applying QSPR to estimate the efficiency of corrosion inhibitors, the experimental conditions have a strong influence on the values obtained [39–42] and the definition of property (efficiency of corrosion inhibitors) in terms of experimental conditions is an essential part of the approach, which implies that the data must be obtained according to a single experimental protocol. In this context, in the present work, we were constrained to limit ourselves to the six molecules published experimentally, each taken at 4 different concentrations so that the number of individuals rises to 24 while carefully respecting the experimental conditions for obtaining these efficiencies. The aim of the present study is to perform a detailed quantum chemical as well as statistical calculations on molecular electronic and structural properties of six bis-benzimidazole molecules denoted hereafter BBI, MBBI, EBBI, BBBI, HBBI, OBBI, collected in Table 1, already studied as mild steel corrosion inhibitors in 1 M HCl in the range of concentration from 10^{-5} to 10^{-3} M with distinguishable efficiencies [43]. On the basis of some studies which has been reported the influence of certain properties in the corrosion inhibition processes [39,40–42]. The present investigation projects to explore the possible correlation between corrosion inhibition efficiency and a number of molecular indices such as E_{HOMO}, E_{LUMO}, μ, V_c, *Log P* and *M*, by means of AM1, HF and DFT as quantum methods, along with the statistical models MLR, PLS and MPR, by presenting their principles as well as the various tools used for their implementation and evaluation: experimental databases, descriptors and data analysis tools.

2. Computational methodology

2.1 Quantum chemical calculations

Theoretically, the quantum chemistry is the most widespread method to study the phenomenon of corrosion inhibition. It ensures the optimized structure and brings out the descriptors which relate the corrosion inhibiting character, in order to have some insights into the experimental results as well as the complex process of corrosion inhibition. In this context, different methods and several bases were used. Depending on the nature of the theoretical study undertaken and the calculated properties, the most popular methods were: the semi-empirical method (AM1), the Hartree-Fock method (HF), the Post HF method (MP2) and the density functional theory method DFT/ B3LYP. The most tested bases were: 3-21G; 6-31G; 6-311G; 6-31G (d, p); 6-31+G (d, p); 6-31++G (d, p); 6-311G (d, p); 311+G (d, p) and 311++G (d, p) as usually reported in the literature [45–53].

Theoretical parameters such as the energies of the highest occupied and lowest unoccupied molecular orbitals (E_{HOMO} and E_{LUMO}), the energy gap (Δ*E*), the dipole moment (μ), the molecular weight (*M*), the logarithm of the partition coefficient (log *P*), the absolute electronegativity (χ), the global hardness (η), the ionization potential (*IP*), the electron affinity (*EA*) and the fraction of electrons transferred from the inhibitor molecule to the metal surface (Δ*N*), were determined in the first stage of this work.

The ionization potential *IP* and the electron affinity *EA* are related to E_{HOMO} and E_{LUMO}, respectively through the equations [53]:

$$IP = -E_{HOMO} \tag{1}$$

Table 1
Molecular structures, names and abbreviations of the studied bis-benzimidazole derivative molecules

Structure	Name	Abbreviation
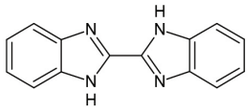	1H,1′H-2,2′-bibenzimidazole	BBI
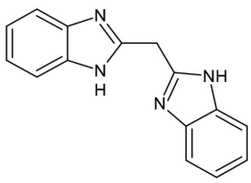	2,2′-methanediylbis(1H-benzimidazole)	MBBI
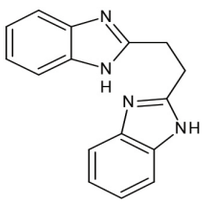	2,2′-ethane-1,2-diylbis(1H-benzimidazole)	EBBI
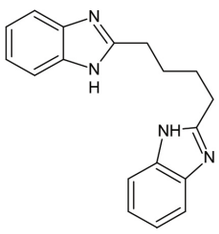	2,2′-butane-1,4-diylbis(1H-benzimidazole)	BBBI
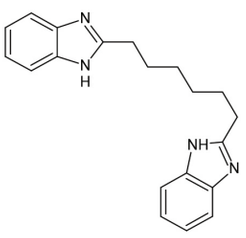	2,2′-hexane-1,6-diylbis(1H-benzimidazole)	HBBI
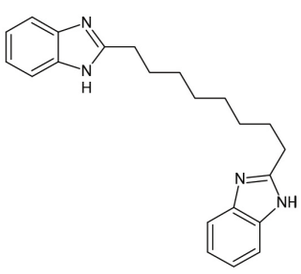	2,2′-octane-1,8-diylbis(1H-benzimidazole)	OBBI

$$EA = -E_{LUMO} \quad (2)$$

The electronegativity χ, the global hardness η and the softness σ were evaluated, based on the finite difference approximation, as linear combinations of the calculated *IP* and *EA* [53]:

$$\chi = \frac{IP + EA}{2} \quad (3)$$

$$\eta = \frac{IP - EA}{2} \quad (4)$$

$$\sigma = \frac{1}{\eta} \tag{5}$$

Moreover, for a reaction of two systems with different electronegativities, the electronic flow will occur from the organic inhibitor with lower electronegativity towards that of higher value (metallic surface), until the chemical potentials are equal [54]. Therefore, the fraction of electrons transferred (ΔN) from the inhibitor derivative to the metallic atom was calculated according to Pearson electronegativity scale [54]:

$$\Delta N = \frac{\chi_{Fe} - \chi_{inh}}{2(\eta_{Fe} + \eta_{inh})} \tag{6}$$

A theoretical value for the electronegativity of bulk iron of χ_{Fe}= 7*eV* and a global hardness of η_{Fe}= *EA* were used, by assuming that for a metallic bulk *IP* = *EA* because they are softer than the neutral metallic atoms [55].

2.2. QSPR calculations

As a second part of this study, the correlation between the calculated theoretical parameters and the experimental corrosion inhibition efficiency E% was studied. Statistically, several linear or non-linear regression models were proposed in the literature in similar studies [36–39]. The choice of a predictive model represents the essential stage for every study. The main QSPR models undertaken in the present study, are as follows:

2.2.1. Multiple linear regression model (MLR)

This model makes it possible to determine the calculated or predicted inhibition efficiency as a function of the theoretical descriptors according to the following Eq. (7):

$$E_{cal}\% = AX_jC_i + B \tag{7}$$

where *B* is a constant, *A* is a quantum chemical index coefficient; X_j is a quantum chemical index characteristic for the molecule j; C_i denotes the inhibitor concentration

2.2.2. Partial least squares regression model (PLS)

PLS regression is a relatively recent model that generalizes and combines features from principal component analysis and multiple regression. It originated from the social sciences (specifically economy, Herman Wold, 1966), but became popular first in chemo-metrics (i.e., computational chemistry) due in part to Herman's son Svante. It was rapidly interpreted in a statistical framework (Frank and Friedman, 1993; Helland, 1990; Höskuldsson, 1988; Tenenhaus, 1998) [56]. It is particularly useful when it is needed to predict a set of dependent variables from a large set of independent variables (i.e., predictors); by the elimination of some predictors (e.g., using step-wise methods), or by performing a principal component analysis (PCA) of the predictors matrix [56]. PLS uses the same model expresses by Eq. (7).

2.2.3. Multiple polynomial regression (MPR)

The multiple polynomial regression (MPR) is considered, in our knowledge, as new model for QSPR methods, notwithstanding the fact that it is used in other domains. It is a homogeneous quadratic polynomial of second degree with a number of variables, based on the semi-empirical QSPR approach. In the field of corrosion inhibition, it is expressed by Eq. (8):

$$\begin{aligned} E_{cal}\% = cst &+ (a_0 + a_1E_{HOMO} + a_2E_{LUMO} \\ &+ a_3\mu + a_4LogP + a_5V_c + a_6M)C_i \\ &+ (b_0E_{HOMO} + b_1E_{LUMO} + b_2\mu \\ &+ b_3LogP + b_4V_c + b_5M)C_i^2 \end{aligned} \tag{8}$$

where a_0, a_1, a_2, a_3, a_4, a_5, a_6, b_0, b_1, b_2, b_3, b_4 and b_5 are quantum chemical index coefficients; E_{HOMO}, E_{LUMO}, μ, log *P*, V_C and *M* are quantum chemical index characterizing the inhibitor molecule.

3. Results and discussion

3.1. Quantum calculation

3.1.1. Molecular geometry

To bring about the quality of the theoretical and statistical results, the geometries of the whole molecules, considered in this work, are fully optimized at AM1, HF and DFT level of theory using the B3LYP functional together with 6-311G basis set in gaseous phase, by means of Gaussian 03 set of programs [57]. The absence of imaginary frequencies in the vibrational spectra proves that the equilibrium structures correspond to the minima energy for each bis-benzimidazole derivative.

The final optimized structures along with the bond lengths are shown in Fig. 1. The pertinent bend lengths are $N_1C_{1'}$, $N_1C_{7'}$, $N_2C_{7'}$, N_2C_6 and C_1C_6 (equivalent to $N_4C_{9'}$, $N_4C_{8'}$, $N_3C_{8'}$, N_3C_{14} and C_9C_{14} respectively), remain almost the same whatever the studied molecule or the method. Hence the optimized structures for all the studied compounds exhibit a similar conformation.

Besides, Table 2 exemplifies the dihedral angles, and similar results are obtained, except for the dihedrals: [N_1, $C_{7'}$, $C_{15'}$, C_8], [C_7, $C_{15'}$, $C_{8'}$, N_4] for MBBI and [N_4, $C_{8'}$, $C_{16'}$, C_{15}], [$C_{16'}$, $C_{15'}$, $C_{7'}$, N_1] for EBBI. Accordingly, the choice of the appropriate method cannot be made based on the structural parameters such as bond distances and dihedral angles got from AM1, HF and DFT/B3LYP methods. However, it should be noted that HF calculations tend to underestimate the lengths of most bonds.

Thus, the structural parameters cannot constitute a criterion that can define the best method to conduct the theoretical study. However, the CPU (central processing unit) results, also reported in Table 3, show that the AM1 method is the fastest of the three methods. The analysis of these results shows that the CPU related to the DFT/B3LYP method is relatively higher in comparison with the HF method, because of the consideration of electronic correlation that this method makes during the calculation of molecular systems.

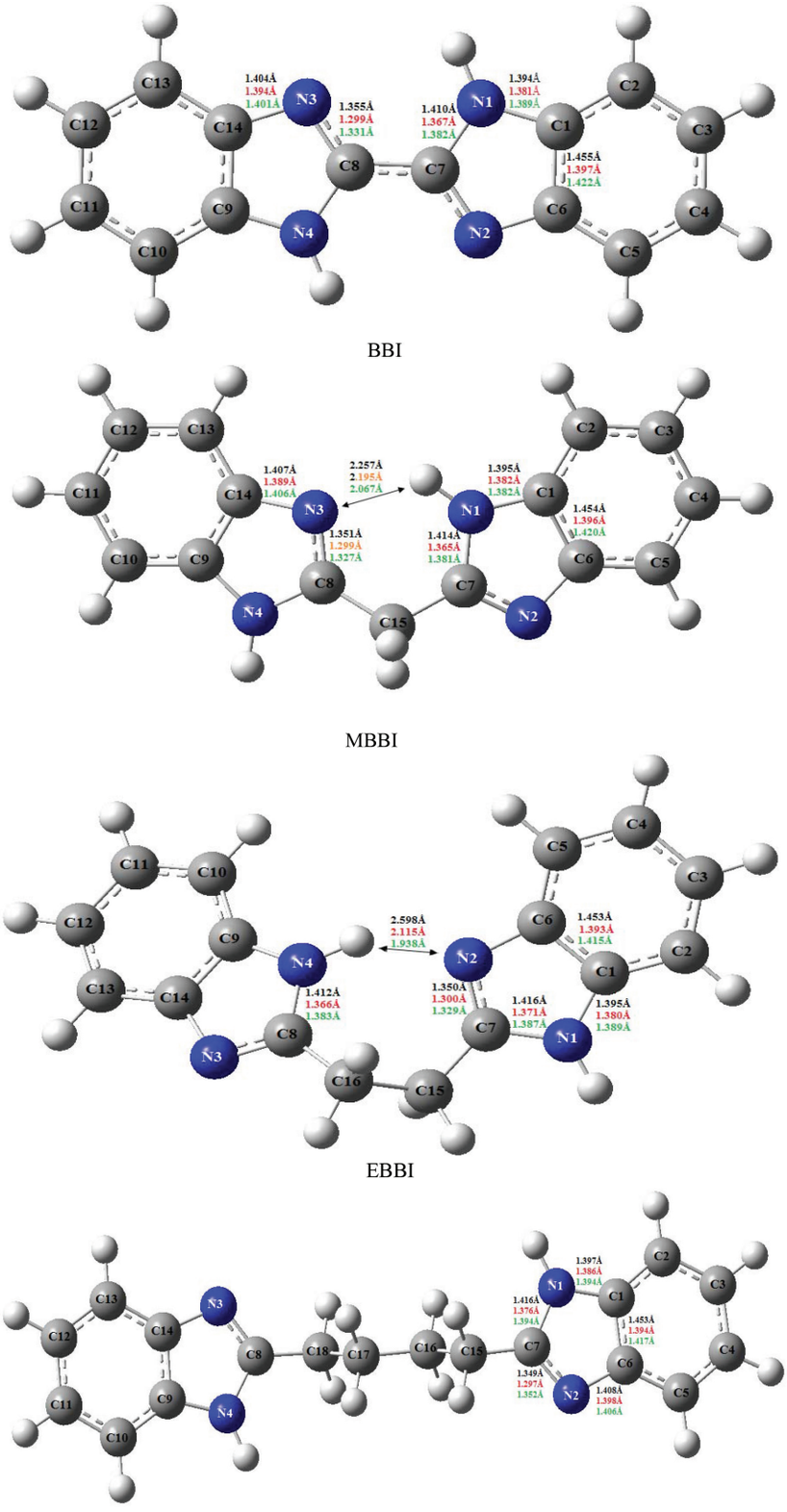

Fig. 1. Optimized molecular structures and bond lengths of the studied inhibitors calculated in gas phases at AM1 (black), HF (red) and B3LYP/6-311G (green).

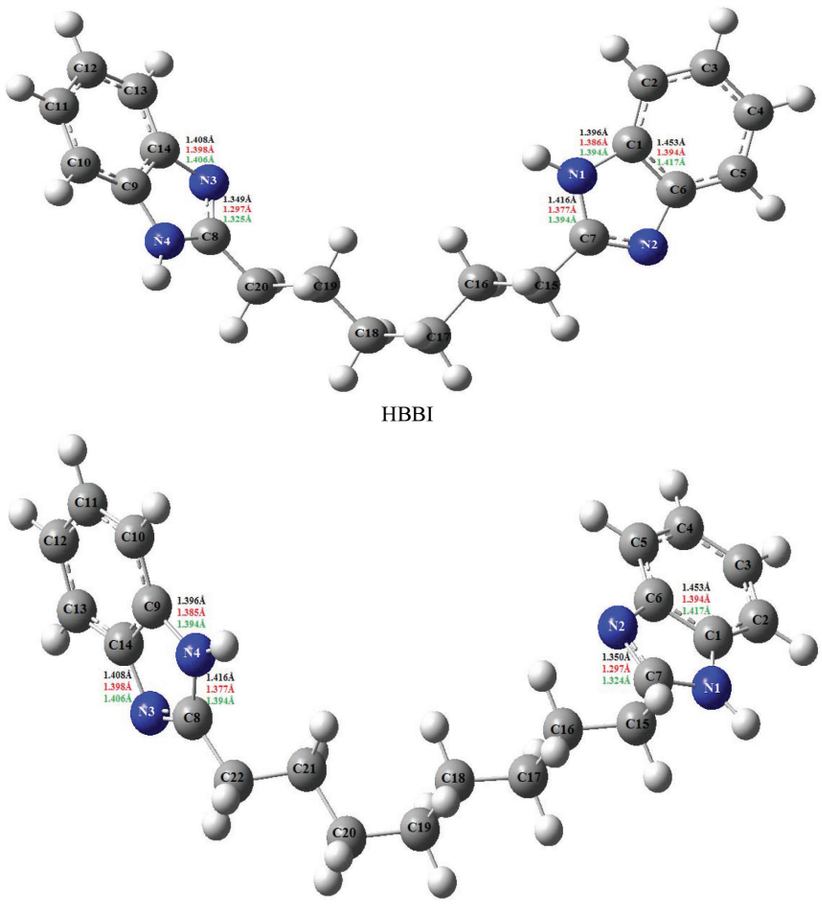

Fig. 1. (*Continued*).

With the aim of discriminating between these three methods and to keep only one, we based ourselves on the following magnitudes CPU, E_T and ΔE. Indeed, AM1 can be quickly ruled out due to the positive values of the obtained total energy despite the extremely low time of calculation, CPU. Furthermore, the energy gap is very high which reflects an extremely low reactivity of the whole molecules. Besides, the comparable study of both methods HF and DFT reveals that the total energy presents usually the minima for the DFT method with a calculation time which remains lower for the small molecules to become higher when the molecular size is more important. Further, the energies gap obtained with DFT are always weaker than those stemming from HF. In this established fact, DFT thus gets ready as a successful method of choice to lead the rest of the theoretical study.

3.1.2. Global Molecular reactivity descriptors

The E_{HOMO} are the highest values at DFT in comparison with those of AM1 and HF methods. E_{HOMO} is often associated with the electron donating ability of the molecule, Therefore, high value of E_{HOMO} indicates high tendency of the molecule to donate electrons to appropriate acceptor which is an empty molecular orbital of low energy.

The E_{LUMO} are the lowest values at DFT in comparison with those of AM1 and HF methods. Therefore, the energy of the lowest unoccupied molecular orbital indicates the ability of the molecule to accept electrons. A low value of E_{LUMO} indicate high tendency of the molecule to accept electrons from the metal surface [58]. Therefore, for all the previous reasons, the AM1 and HF methods are ruled out. Whereas, the DFT appears as the suitable theoretical method in the present study.

The results presented in Table 3 allowed to classify the undertaken inhibitors into two groups: the first one is (BBI and MBBI) namely; group A, the second is (EBBI, BBBI, HBBI and OBBI) namely; group B. For group A, the obtained values of E_{HOMO} corresponding to each organic inhibitor indicate that E_{HOMO} (BBI) ≈ E_{HOMO} (MBBI). In the opposite, BBI have the lowest E_{LUMO} (–1.752 eV) when compared to MBBI (–1.040 eV), which indicate a better capability for BBI to accept electrons from the mild steel surface. For group B, it can be clearly seen that E_{HOMO} and E_{LUMO} follow the order as: OBBI > HBBI > EBBI > BBBI, for HOMO and BBBI > HBBI > EBBI > OBBI, for LUMO. The highest value of E_{HOMO} and the lowest E_{LUMO} of OBBI indicates the best inhibition efficiency than the other compounds.

The gap between the E_{HOMO} and E_{LUMO} energy levels of the molecules constitutes an important parameter of reactivity

Table 2
Pertinent dihedral angels, in degree, of the studied inhibitors calculated at AM1, HF and DFT/B3LYP in gas phases

Inhibitor	Dihedral angle	AM1	HF	DFT/B3LYP
BBI	[N_1, C_7, C_8, N_4]	179.99	179.99	180.00
MBBI	[N_1, C_7, C_{15}, C_8]	55.88	32.78	27.71
	[C_7, C_{15}, C_8, N_4]	106.25	147.13	152.27
EBBI	[N_4, C_8, C_{16}, C_{15}]	97.37	65.75	57.57
	[C_8, C_{16}, C_{15}, C_7]	71.41	79.86	79.43
	[C_{16}, C_{15}, C_7, N_1]	168.37	160.63	145.38
BBBI	[N_1, C_7, C_{15}, C_{16}]	72.59	73.99	76.21
	[C_7, C_{15}, C_{16}, C_{17}]	178.39	177.89	177.67
	[C_{15}, C_{16}, C_{17}, C_{18}]	179.99	180.00	179.97
	[C_{16}, C_{17}, C_{18}, C_8]	178.41	177.89	177.65
HBBI	[N_1, C_7, C_{15}, C_{16}]	59.89	67.03	65.70
	[C_7, C_{15}, C_{16}, C_{17}]	174.85	176.68	175.74
	[C_{15}, C_{16}, C_{17}, C_{18}]	177.71	178.01	179.93
	[C_{16}, C_{17}, C_{18}, C_{19}]	78.96	69.18	70.01
	[C_{17}, C_{18}, C_{19}, C_{20}]	178.46	177.97	178.96
	[C_{18}, C_{18}, C_{20}, C_8]	179.58	179.16	179.58
OBBI	[N_4, C_8, C_{22}, C_{21}]	59.65	66.39	66.29
	[C_8, C_{22}, C_{21}, C_{20}]	175.11	177.41	176.79
	[C_{22}, C_{21}, C_{20}, C_{19}]	180.00	177.37935	178.83
	[C_{21}, C_{20}, C_{19}, C_{18}]	78.720	68.45	68.63
	[C_{20}, C_{19}, C_{18}, C_{17}]	178.74	176.89	177.58
	[C_{19}, C_{18}, C_{17}, C_{16}]	178.40	179.07	178.48
	[C_{18}, C_{17}, C_{16}, C_{15}]	177.67	179.35	179.21
	[C_{17}, C_{16}, C_{15}, C_7]	73.70	71.52	70.52

for an inhibitor molecule towards adsorption on to the metallic surface. As ΔE decreases, the reactivity of the molecule increases, leading to an increase of E %. Indeed, lower values of the energy difference represents an indicator of good inhibition efficiency, because the energy to remove an electron from the last occupied orbital to the lower unoccupied orbital will be low [59]. The value of ΔE, indicated in Table 2, show that; BBI < MBBI for group A and OBBI < HBBI < BBBI < EBBI for group B, which suggests that the inhibitors BBI and OBBI have the lowest energy gap for the two groups, and hence highest reactivity in comparison to the other compounds, could have better performance as corrosion inhibitor which is in agreement with the experimental values of E %.

For the dipole moment, there is an inconsistent, in the literature, on the correlation between the dipole moment and inhibition efficiency [60]. However, it is well reported that higher value of dipole moment probably increases the adsorption of chemical compound on metal surface [61] which increases the contact area between the molecule and surface of iron then increasing the corrosion inhibition ability of inhibitors. The results indicate that the values of μ do not follow a well-defined order; which implies that μ is not a very determinant parameter for E %, in this study.

Hardness and softness are the basic chemical concepts, called the reactivity descriptors which have been theoretically justified within the framework of density functional theory (DFT) [62]. They are the important properties to measure the molecular stability and reactivity. A hard molecule has a large energy gap and a soft molecule has a small energy gap [52]. Table 4 shows the order of hardness as: BBI < MBBI for group A and OBBI < HBBI < BBBI < EBBI for group B and the order of softness as: BBI > MBBI for group A and OBBI > HBBI > BBBI > EBBI for group B, which implies that BBI have the highest inhibition efficiency when compared to MBBI, whereas OBBI have also a highest E % in comparison with HBBI, BBBI and EBBI.

The number of electrons transferred ΔN is also calculated and reported in Table 4. Values of ΔN show that the inhibition efficiency resulting from electron donation agrees with Lukovits's study [63]. Generally, if ΔN < 3.6, the inhibition efficiency increases by increasing electron-donating ability of these inhibitors to donate electrons to the metal surface. From results of Table 4, ΔN increases in the following order: BBI > MBBI for group A and OBBI > HBBI > BBBI > EBBI for group B. The results indicate that ΔN values correlates strongly with experi-

Table 3
Quantum chemical parameters of compounds BBI to OBBI using AM1, HF and DFT calculations

Inhibitor	Parameter	AM1	HF	DFT/B3LYP	Log P	M/g·mol^{-1}	V_c/cm^3·mol^{-1}
BBI	E_{HOMO} (eV)	–8.665	–8.024	–6.090	2.019	234.262	681.5
	E_{LUMO} (eV)	–0.740	1.876	–1.752			
	ΔE (eV)	7.925	9.900	4.337			
	μ (D)	0.001	0.000	0.001			
	E_T (eV)	5.899	–20499.252	–20631.539			
	CPU	2 min 21 s	1 h 54 min 1 s	59 min 5 s			
MBBI	E_{HOMO} (eV)	–8.893	–8.187	–6.020	3.838	248.289	737.5
	E_{LUMO} (eV)	–0.230	2.856	–1.040			
	ΔE (eV)	8.663	11.043	4.980			
	μ (D)	1.839	4.220	4.768			
	E_T (eV)	5.582	–21560.678	–21700.711			
	CPU	6 min 44 s	4 h 20 min 27 s	4 h 15 min 3 s			
EBBI	E_{HOMO} (eV)	–8.879	–8.024	–6.238	2.776	262.316	793.5
	E_{LUMO} (eV)	–0.070	2.856	–0.658			
	ΔE (eV)	8.809	10.88	5.58			
	μ (D)	0.001	6.154	6.269			
	E_T (eV)	5.328	–22603.2	–22769.906			
	CPU	3 min 12s	3 h 53 min 54 s	5 h 30 min 41 s			
BBBI	E_{HOMO} (eV)	–8.893	–8.323	–6.266	3.610	290.370	905.5
	E_{LUMO} (eV)	–0.016	3.155	–0.688			
	ΔE (eV)	8.877	11.478	5.578			
	μ (D)	0.008	0.001	0.023			
	E_T (eV)	4.738	–24745.036	–24908.417			
	CPU	4 min 32 s	5 h 51 min 46 s	7 h 14 min 27 s			
HBBI	E_{HOMO} (eV)	–8.855	–8.268	–6.198	4.44	318.424	1017.5
	E_{LUMO} (eV)	0.022	3.182	–0.662			
	ΔE (eV)	8.878	11.45	5.536			
	μ (D)	1.7570	5.267	5.104			
	E_T (eV)	4.209	–26867.969	–27046.965			
	CPU	6 min 42s	8 h 6 min 23 s	9 h 51 min 2 s			
OBBI	E_{HOMO} (eV)	–8.840	–8.187	–6.134	5.279	346.478	1129.5
	E_{LUMO} (eV)	0.033	3.236	–0.622			
	ΔE (eV)	8.873	11.432	5.512			
	μ (D)	2.482	6.556	6.905			
	E_T (eV)	3.645	–28990.929	–29185.501			
	CPU	10 min 7s	10h 59 min 1s	15 h 36 min 47 s			

mental inhibition efficiencies. Thus, the highest fraction of electrons transferred is associated with the best inhibitor (BBI) for group A and (OBBI) for group B, while the lowest fraction is associated with the inhibitor that has the least inhibition efficiency (MBBI) for group A and (EBBI) for group B.

It is to be concluded from the evolution of the considered global descriptors that ΔE, η, σ and ΔN follow the tendency of experimental inhibition efficiencies of the studied molecules. They can explain the molecular reactivity in terms of corrosion inhibition efficiency. On the contrary, E_{HOMO}, $E_{LUMO,}$ μ and χ do not follow the same order of the

Table 4
Quantum chemical parameters of compounds BBI to OBBI using DFT calculations

Inhibitor	PI/eV	EA/eV	χ/eV	η/eV	σ/eV^{-1}	ΔN	E_{exp}%
BBI	6.090	1.752	3.921	2.169	0.461	0.709	88.6
MBBI	6.020	1.040	3.53	2.49	0.402	0.696	82.1
EBBI	6.238	0.658	3.448	2.79	0.358	0.631	28.1
BBBI	6.266	0.688	3.477	2.789	0.359	0.636	52.3
HBBI	6.198	0.662	3.43	2.768	0.361	0.644	88.8
OBBI	6.134	0.622	3.378	2.756	0.362	0.657	90.2

experimental corrosion inhibition effect of the molecular derivatives. Accordingly, these last descriptors are not representing indexes in the description of the corrosion inhibition process.

Experimentally, the comparative study of the inhibition power shows that the inhibition efficiency decreases as the number n of methylene group of the junction between the two benzimidazole nuclei increases from $n = 0$ to $n = 2$; it reaches its minimum value at $n = 2$ (EBBI). And it increases again, from $n = 4$ to reach its maximum value at $n = 8$ (OBBI). Consequently, the comparison between the experimental and the theoretical results shows that there is a concordance between them. In can be concluded that the quantum study can describe microscopically the evolution of the chemical system at the metal/solution interface and allows giving some insights into the experimental results.

3.2. QSPR study

3.2.1. Statistical analysis

3.2.1.1. Principle of QSPR analysis

Taking into account the complexity of the corrosion inhibition process, the regression analysis is used to correlate quantum chemical parameters and inhibitor concentrations (C_i) with the efficiency E%. It is a statistical technique used to study the relationship between one dependent variable and several independent variables that minimizes the difference between experimental and predicted values using the least-squares method, which consists on minimizing the residual sum square. This implies an analysis of variance, by decomposing the total variance SS_T, which is measured by the sums of squares of the sample, into two partial variances: the explanatory variance (SS_{reg}) and the residual variance (SS_{res}), and these two variances are compared.

$$SS_T = SS_{reg} + SS_{res} \tag{9}$$

A specific indicator allows translating the explained variance by the model, it is the coefficient of determination, and its formula is as follows:

$$R^2 = \frac{SS_{reg}}{SS_T} = 1 - \frac{SS_{res}}{SS_T} \tag{10}$$

Indeed, R^2 is certainly a relevant indicator, it presents sometimes-boring defect; it tends to increase automatically when other variables are added in the model. Therefore, it is ineffective when comparing models containing a different number of variables. It is in this case recommended to use the adjusted coefficient of determination which is corrected by the degree of freedom (DF):

$$R^2_{adj} = 1 - \frac{SS_{res}}{SS_T} \times \frac{N-1}{N-P-1} = 1 - \frac{N-1}{N-P-1} \times (1-R^2) \tag{11}$$

3.2.1.2. Regression equations

Using the statistical software Minitab 16 the values of the different regression models are as follows:

a. Multiple Linear Regression MLR
For AM1 quantum calculations

$$E_{cal}\% = -105.148 + 0.07C_i - 16.115E_{HOMO} - 47.675LogP + 35.55\mu + 0.612M \tag{12}$$

$R^2 = 0.97$

For HF/6-311G quantum calculations

$$E_{cal}\% = -1987.837 + 0.07C_i - 271.006E_{HOMO} - 113.750E_{LUMO} + 12.172\mu + 0.448M \tag{13}$$

$R^2 = 0.97$

For DFT-B3LYP/6-311G quantum calculations

$$E_{cal}\% = -2156.230 + 0.07C_i - 332.709E_{HOMO} - 106.976E_{LUMO} + 11.886LogP + 14.483M \tag{14}$$

$R^2 = 0.97$

b. Partial Least Squares Regression (PLS)
For AM1 quantum calculations

$$E_{cal}\% = -82.057 + 0.066C_i - 16.122E_{HOMO} - 2.368E_{LUMO} - 44.647LogP + 34.663\mu \tag{15}$$

$R^2 = 0.96$

For HF/6-311G quantum calculations

$$E_{cal}\% = 1129.5 + 0.046C_i - 133.193E_{HOMO} - 16.718E_{LUMO} + 5.498LogP + 5.04\mu \quad (16)$$

$R^2 = 0.96$

For DFT-B3LYP/6-311G quantum calculations

$$E_{cal}\% = 1785.228 + 0.08C_i - 272.131E_{HOMO} - 95.104E_{LUMO} + 6.849LogP + 13.5\mu \quad (17)$$

$R^2 = 0.96$

A first analysis of the statistical parameters, in particular the coefficient of determination R^2, reveals that the two models MLR and PLS are very efficient. However, the diagnosis of residue diagrams shows the lack of a quadratic term in the two models.

For this purpose, we have proposed a multiple polynomial regression (MPR) with quadratic terms as a suitable concept for better modeling the inhibition efficiency of bis-benzimidazole derivatives.

c. Multiple polynomial regression (MPR)

For AM1 quantum calculations:

$$\begin{aligned} E_{cal}\% = {} & -67.6 - 11.8E_{HOMO} - 21.3E_{LUMO} \\ & - 37.5LogP + 0.15V_c + 29.9\mu \\ & - 0.557E_{HOMO} \times C_i + 2.44E_{LUMO} \\ & \times C_i + 0.767\mu \times C_i - 1.25LogP \\ & \times C_i + 0.005E_{HOMO} \times C_i^2 - 0.022E_{LUMO} \\ & \times C_i^2 - 0.007\mu \times C_i^2 + 0.0116LogP \times C_i^2 \end{aligned} \quad (18)$$

$R^2 = 0.99$

For HF/6-311G quantum calculations

$$\begin{aligned} E_{cal}\% = {} & -1078 - 154E_{HOMO} - 85.2E_{LUMO} \\ & - 1.1LogP + 0.12V_c + 9.54\mu - 20.5E_{HOMO} \\ & \times C_i - 4.88E_{LUMO} \times C_i + 0.587\mu \times C_i \\ & - 0.345LogP \times C_i + 0.617V_c \times C_i - 2.45M \\ & \times C_i + 0.177E_{HOMO} \times C_i^2 + 0.042E_{LUMO} \\ & \times C_i^2 - 0.005\mu \times C_i^2 + 0.02M \times C_i^2 \end{aligned} \quad (19)$$

$R^2 = 0.99$

For DFT-B3LYP/6-311G quantum calculations

$$\begin{aligned} E_{cal}\% = {} & -860 - 121E_{HOMO} - 76.4E_{LUMO} \\ & - 0.26LogP + 0.09V_c + 9.34\mu - 20.1E_{HOMO} \\ & \times C_i - 3.02E_{LUMO} \times C_i + 0.59\mu \times C_i + 0.97LogP \times C_i \\ & + 0.47V_c \times C_i - 1.94M \times C_i + 0.174E_{HOMO} \\ & \times C_i^2 + 0.026E_{LUMO} \times C_i^2 - 0.005\mu \times C_i^2 \\ & - 0.008LogP \times C_i^2 + 0.01M \times C_i^2 \end{aligned} \quad (20)$$

$R^2 = 0.99$

The predicted E_{cal} % values calculated from the Eqs. (12)–(20) using the MLR, PLS and MPR models are given in Table 5 along with the residual errors (RE) and the average (Av) of the whole equations proposed for AM1, HF and DFT.

The comparison between experimental and calculated efficiency values is represented in Figs. 2–4.

From Figs. 2–4 it seems that the value of the calculated efficiencies E_{cal} % obtained from the MLR, PLS and MPR models by DFT are in very good agreement with the experimental efficiencies E_{exp} % values and show a good correlation between the corrosion inhibition efficiency and the molecular structure in comparison with those obtained by the AM1 and HF methods.

Moreover, in order to decide on the best method for calculating the quantum descriptors as well as the top regression method for modeling the inhibition efficiency of the bis-benzimidazole derivatives, an analysis of the variances was carried out.

3.2.2. Correlation and variance analysis

3.2.2.1. Correlation analysis

For MLR model, statistical characteristics of the obtained Eq. (17) are: $N = 24$; $r = 0.98$; $R^2 = 0.97$ and $R^2_{adj} = 0.97$; $R^2_{pred} = 0.96$; *PRESS= 556.92* and *SD* = 2.34, where *R* is the correlation coefficient; R^2 is the determination coefficient; R^2_{adj} is the adjusted determination coefficient; *SD* is the standard deviation and N is the number of observations.

For PLS model, statistical characteristics of the obtained Eq. (20) are: $N = 24$; $r = 0.97$; $R^2 = 0.97$; $R^2_{adj} = 0.97$; $R^2_{pred} = 0.95$; *PRESS= 601.29* and *SD*= 2.46.

Correlation matrix between the six descriptors is shown in Table 6.

For MPR model, statistical characteristics of the obtained Eq. (23) are: $N = 24$, $r = 0.99$, $R^2 = 0.99$, $R^2_{adj} = 0.99$; $R^2_{pred} = 0.97$; *PRESS= 441.17* and *SD* = 0.32.

MLR, PLS and MPR regression coefficients using DFT-B3LYP/6-311G calculations are represented in Table 7.

The characteristics values of models (r, R^2 and R^2_{adj}) demonstrate that the MLR, PLS and MPR models explain the inhibition efficiency (*E*%) with a high level of significance. However, to choose the appropriate model, it was necessary to compare the prediction indicators of the studied regressions. Effectively, the predicted determination coefficient (R^2_{pred}) and the predicted residual error sum of squares (PRESS) are the most used parameters to evaluate the quality of prediction of statistical models. So, the obtained values of these parameters show that the MPR is the more significant predictive model due to its low PRESS which equals 441.17 value and high predicted determination coefficient $R^2_{pred} = 0.97$.

To confirm the predictive power of the selected models, the correlation between experimental and predicted efficiency is illustrated in Figs. 5–7.

According to the statistical results, we generally notice that the inhibition efficiency is directly connected to the selected molecular descriptors. From the correlation matrix (Table 6) and regression coefficients (Table 7), we note that critical volume (V_c), and molar mass (*M*), are perfectly cor-

Table 5
E_{exp}% vs E_{cal}% obtained by (MLR, PLS and MPR) models, proposed for AM1, HF/6-311G and DFT-B3LYP/6-311G along with the average and the residual error

Inh.	10^5 C_i/M	E_{exp}%	AM1			HF/6-311G			DFT-B3LYP/6-311G			Average (Av)			Residual Error (RE)		
			E_{cal}% MLR	E_{cal}% PLS	E_{cal}% MPR	E_{cal}% MLR	E_{cal}% PLS	E_{cal}% MPR	E_{cal}% MLR	E_{cal}% PLS	E_{cal}% MPR	Av. -1	Av.- 2	Av.- 3	RE.-1	RE.-2	RE.-3
BBI	1	78.5	81.65	81.88	78.07	81.71	66.24	78.14	81.56	80.52	78.14	81.64	76.21	78.12	– 3.14	2.29	0.38
	5	81.3	81.93	82.15	81.98	81.99	79.34	81.98	81.84	80.78	81.98	81.92	80.76	81.98	– 0.62	0.54	– 0.68
	10	86.7	82.28	82.47	86.45	82.34	79.52	86.38	82.19	87.10	86.38	82.27	83.03	86.40	4.43	3.67	0.30
	100	88.6	88.62	88.38	88.60	88.68	79.76	88.60	88.53	88.71	88.60	88.61	85.62	88.60	– 0.01	2.98	0.00
MBBI	1	65.8	72.56	74.67	65.68	72.94	83.94	65.53	73.10	68.98	65.53	72.87	75.86	65.58	– 7.07	–10.06	0.22
	5	71.2	72.84	74.94	71.71	73.22	75.10	71.70	73.38	72.31	71.70	73.15	74.12	71.70	– 1.95	– 2.92	– 0.50
	10	79	73.19	75.26	78.61	73.57	75.28	78.76	73.73	76.44	78.76	73.50	75.66	78.71	5.50	3.34	0.29
	100	82.1	79.53	74.17	82.10	79.91	79.70	82.10	80.08	78.29	82.10	79.84	77.39	82.10	2.26	4.71	– 0.00
EBBI	1	22.7	23.60	22.96	22.90	23.52	29.99	22.67	22.71	25.03	22.67	23.28	25.99	22.75	– 0.58	– 3.29	– 0.05
	5	24.57	23.88	23.22	24.64	23.80	29.99	24.63	22.99	24.12	24.63	23.56	25.78	24.63	1.01	– 1.21	– 0.06
	10	26.9	24.24	23.55	26.63	24.15	30.18	26.87	23.34	27.45	26.87	23.91	27.06	26.79	2.99	– 0.16	0.11
	100	28.1	30.58	29.45	28.10	30.49	37.47	28.10	29.68	29.43	28.10	30.25	32.12	28.10	– 2.15	– 4.02	– 0.00
BBBI	1	39.3	44.05	44.24	39.53	44.24	34.59	39.67	45.33	37.46	39.67	44.54	38.76	39.62	– 5.24	0.54	– 0.32
	5	44.5	44.33	44.50	43.79	44.52	37.05	43.80	45.61	42.73	43.80	44.82	41.43	43.80	– 0.32	3.07	0.70
	10	48.2	44.68	44.83	48.68	44.87	37.24	48.53	45.96	46.06	48.53	45.17	42.71	48.58	3.03	5.49	– 0.38
	100	52.3	51.02	46.73	52.30	51.21	41.65	52.30	52.30	56.05	52.30	51.51	48.14	52.30	0.79	4.16	0.00
HBBI	1	76.6	82.98	82.49	76.55	81.34	71.65	76.52	82.58	86.54	76.52	82.30	80.23	76.53	– 5.70	– 3.63	0.07
	5	82.4	83.27	74.75	82.55	81.63	93.02	82.55	82.86	86.86	82.55	82.59	84.88	82.55	– 0.19	– 2.48	– 0.15
	10	89.5	83.62	83.08	89.39	81.98	79.76	89.43	83.21	81.12	89.43	82.94	81.32	89.42	6.56	8.18	0.08
	100	88.8	89.96	88.98	88.80	88.32	79.70	88.80	89.55	83.29	88.80	89.28	83.99	88.80	– 0.48	4.81	–0.00
OBBI	1	82.2	85.92	85.70	82.96	87.04	86.09	83.09	85.51	79.02	83.09	86.16	83.60	83.05	– 3.96	– 1.40	– 0.85
	5	89.2	86.20	85.97	87.52	87.32	92.60	87.53	85.79	85.85	87.53	86.44	88.14	87.53	2.76	1.06	1.67
	10	91.8	86.55	86.30	92.72	87.67	92.60	92.58	86.14	86.28	92.58	86.79	88.39	92.63	5.01	3.41	– 0.83
	100	90.2	92.89	92.20	90.19	94.01	97.20	90.20	92.49	86.88	90.20	93.13	92.09	90.20	– 2.93	– 1.89	0.00

Av. -1: Average of the three obtained MLR equations proposed for AM1, HF and DFT calculations.
Av. -2: Average of the three obtained PLS equations proposed for AM1, HF and DFT calculations.
Av. -3: Average of the three obtained MPR equations proposed for AM1, HF and DFT calculations.
RE.-1: Residual error between the average (Av. -1) and the experimental inhibition efficiency.
RE.-2: Residual error between the average (Av. -2) and the experimental inhibition efficiency.
RE.-3: Residual error between the average (Av. -3) and the experimental inhibition efficiency.

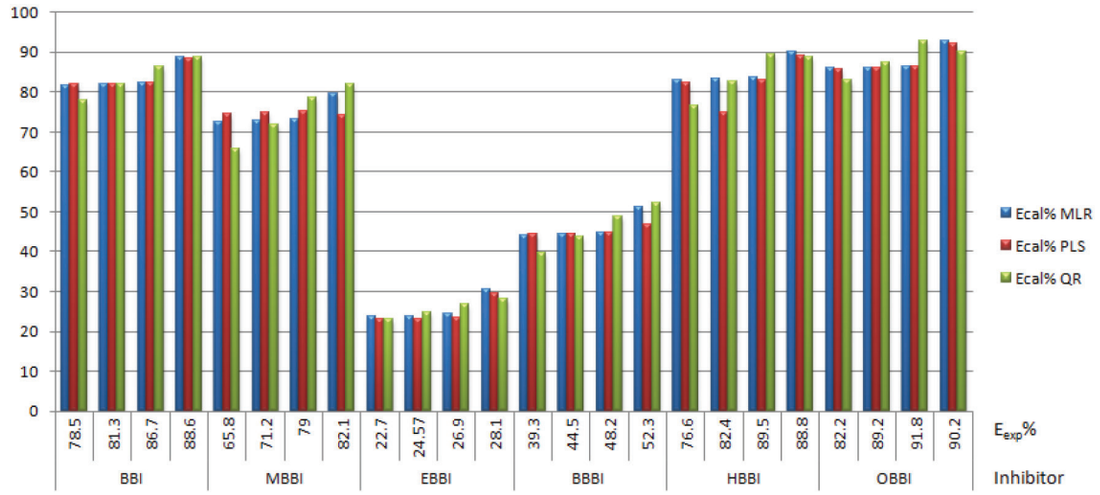

Fig. 2. E_{exp} % and E_{cal} % obtained by (MLR, PLS and MPR) models Eqs. (12), (15), (18) proposed of compounds BBI–OBBI using AM1 calculations.

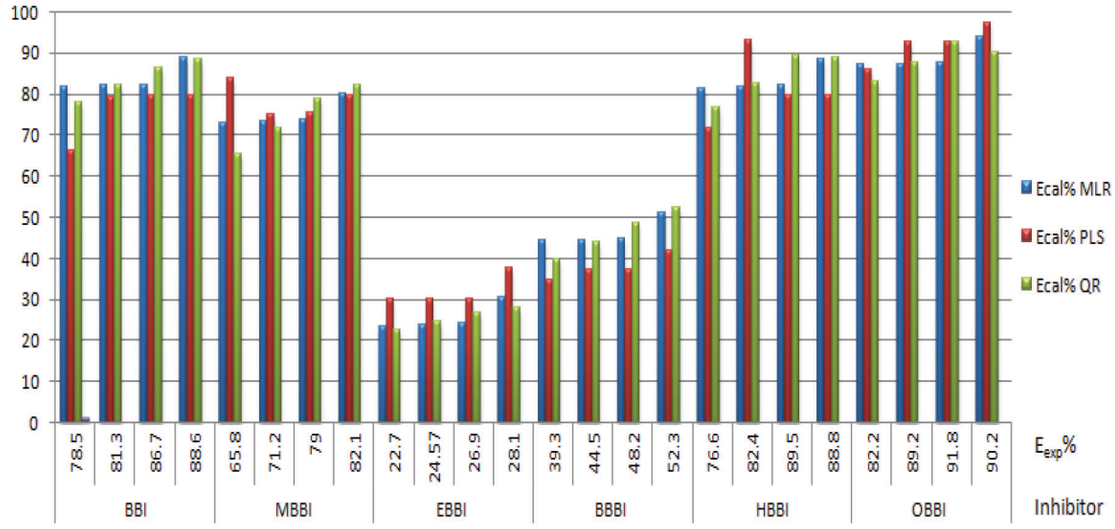

Fig. 3. E_{exp} % and E_{cal} % obtained by (MLR, PLS and MPR) models Eqs. (13), (16), (19) proposed of compounds BBI– OBBI using HF/6-311G calculation.

related (r = 1.000), and have a negligible regression coefficient, whose value tends to 0, which implies that these both variables are redundant, and have low representations in the explanation of the three models. In fact, they can be removed. Contrary, the E_{HOMO}, E_{HOMO}, log P and μ descriptors have significant regression coefficients and a very important contribution. Furthermore, Fig. 8 exemplifies the residual errors (RE) versus the observation in order to highlight the presence or not of a systematic error in developing the three QSPR models (MLR, PLS and MRP) by using AM1, HF and DFT calculation methods.

According to Fig. 8, a random dispersion of the residual errors on both sides of zero testifies that no systemic error exists, as suggested by Jalali-Heravi and Kyani [64]. Accordingly, the three proposed models can be successfully applied to predict the corrosion inhibition efficiency of bis-benzimidazole.

3.2.2.2. *Variance analysis*

For the three undertaken models (MLR, PLS and MPR), the sums of squares *SS*, degrees of freedom *DF*, mean squares *MS*, F_{obs} and p-value associated with F_{sta} are summarized in ANOVA Table 8.

The significance and adequacy of the suggested models are checked by using ANOVA. Indeed, the ANOVA

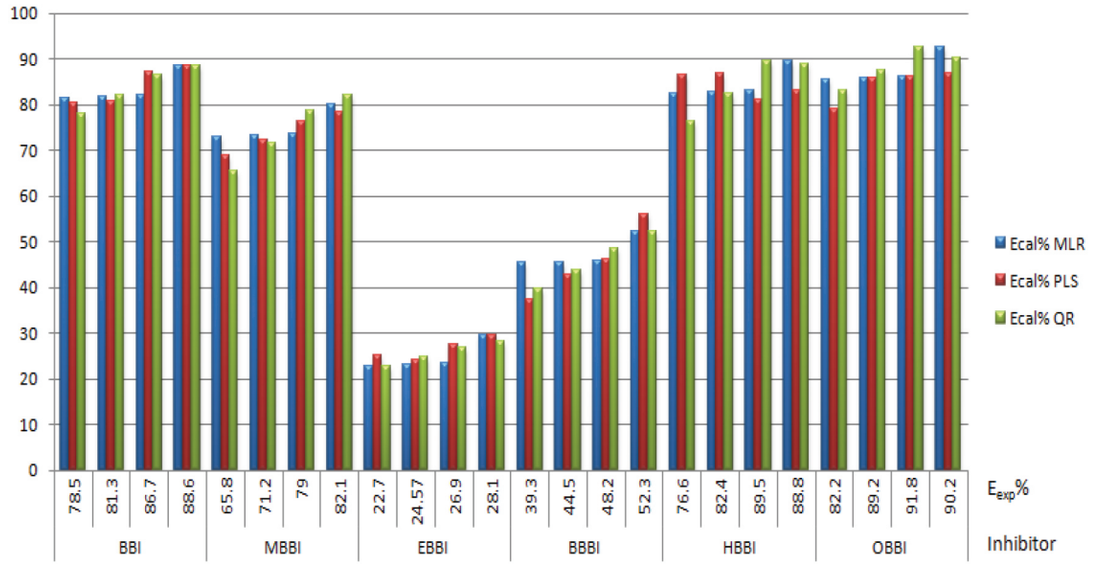

Fig. 4. E_{exp} % and E_{cal} % obtained by (MLR, PLS and MPR) models Eq. ((14), (17), (20)) proposed of compounds BBI– OBBI using B3LYP/6-311G calculations.

Table 6
The correlation matrix between selected descriptors

Variable	10^5 C_i/M	E_{HOMO}/eV	E_{LUMO}/eV	Log P	V_c/cm^{3}mol^{-1}	μ/D	M/g mol^{-1}
10^5 C_i/M	1.000						
E_{HOMO}/eV	0.036	1.000					
E_{LUMO}/eV	−0.119	−0.596	1.000				
Log P	−0.116	−0.109	0.741	1.000			
V_c/cm^{3}mol^{-1}	−0.119	−0.505	0.749	0.859	1.000		
μ/D	−0.051	0.525	0.309	0.746	0.373	1.000	
M/g mol^{-1}	−0.119	−0.505	0.749	0.859	1.000	0.373	1.000

analysis allows us to split the variations into two components; the first one is associated to the regression whereas the second is related to the residual error. The assessment of the ANOVA results for the selected models shows that the variation related to the regression SS_{reg} is largely greater than the residual error SS_{res}; thereby the experimental value F_{obs} is then largely superior to F_{sta} with risk estimations (p-value) significantly inferior to the tolerated risk (5%).

3.2.3. Validation

As is previously indicated, the validity of three models is verified by:

- A higher correlation coefficient R and lower standard error SD, indicate that the models are more reliable.
- The comparison of the residual sum of squares value and the explained sum of squares value $SS_{reg} \rangle SS_{res}$.
- The Fisher test shows that the F_{obs} is much greater than the F_{sta} with a critical probability (p–value < 0. 0001) very clearly below to 5%, which indicates that the null hypothesis is wrong.

Generally, we can conclude, with 95% of confidence, that the models bring globally a significant amount of information, and show that the inhibition efficiency is directly related to the selected molecular descriptors, which means that the good quality and best prediction of selected models. But from Figs. 2–4, and considering the difference between the experimental (E_{exp}%) and the calculated efficiency (E_{cal} %), we notice that, MPR model demonstrate a very significant regression compared with PLS and MLR models which is clearly shown in correlation Figs. 5–7, and demonstrated by the high adjusted determination coefficient R^2_{adj} = 0.99. This later show that about 99% of the variables are consid-

Table 7
MLR, PLS and MPR regression coefficients using DFT-B3LYP/6-311G calculations

Variable	MLR	PLS	MPR
Constant	–1785.229	–2156.230	–860.2
10^5 C_i/M	0.080	0.070	0
E_{HOMO}/eV	–272.131	–332.709	–121.14
E_{LUMO}/eV	–95.105	–106.976	–76.377
Log P	6.850	11.886	–0.262
V_c/cm^3 mol^{-1}	0.017	0	0.09718
μ/D	13.501	14.483	9.344
M/g mol^{-1}	0.068	0	0

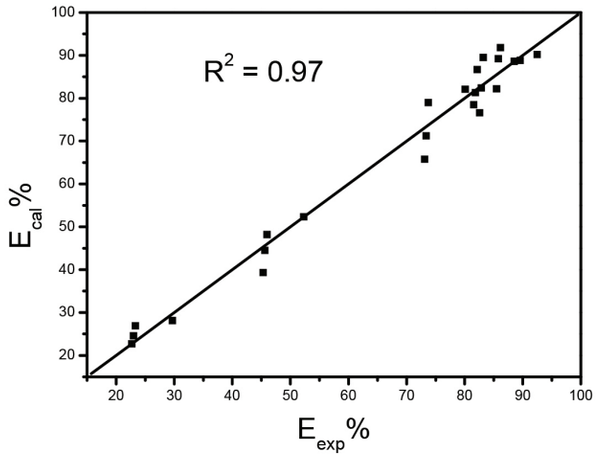

Fig. 5. The experimental vs predicted efficiencies (Eq. (14)) of bis-benzimidazole derivatives.

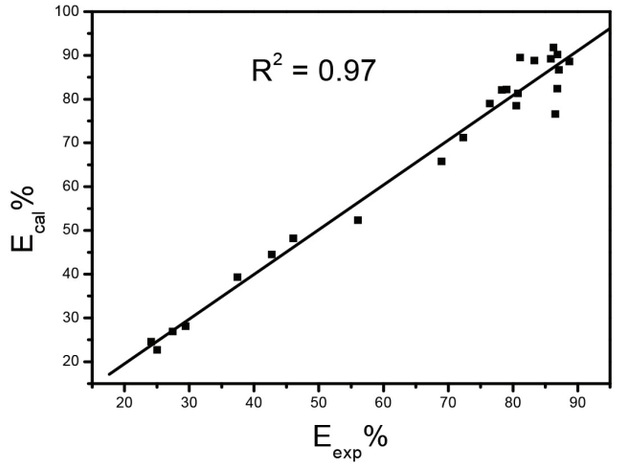

Fig. 6. The experimental vs. predicted efficiencies (Eq. (17)) of bis-benzimidazole derivatives.

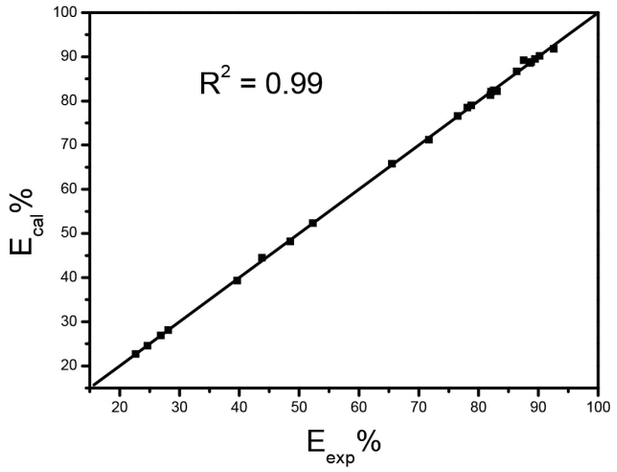

Fig. 7. The experimental vs. predicted efficiencies (Eq. (20)) of bis-benzimidazole derivatives.

ered in the response, and the calculated points are close to the bisector.

The overall comparison between the results of AM1, HF and DFT as quantum methods and the results of MLR, PLS and MPR as statistical results, shows that the choice of the quantum calculation method does not affect much the statistical results. On the other hand, the examination of the results of this study shows that DFT is the best method of quantum study in comparison with AM1 and HF. Similarly, MPR is the most predictive statistic models to study the inhibitors selected in this work.

Finally, a deep analysis of the present results and those reported elsewhere, for the same family of the used molecules [65–73], shows that the benzimidazole derivatives are good corrosion inhibitors. Exceptionally, bis-benzimidazoles perform as efficient inhibitors. They provide valuable insights into the interaction mechanism of the used nitrogenate-heterocyclic inhibitors, also on the relationship between their electronic and lipophilic molecular properties and their corrosion-inhibition ability.

4. Conclusion

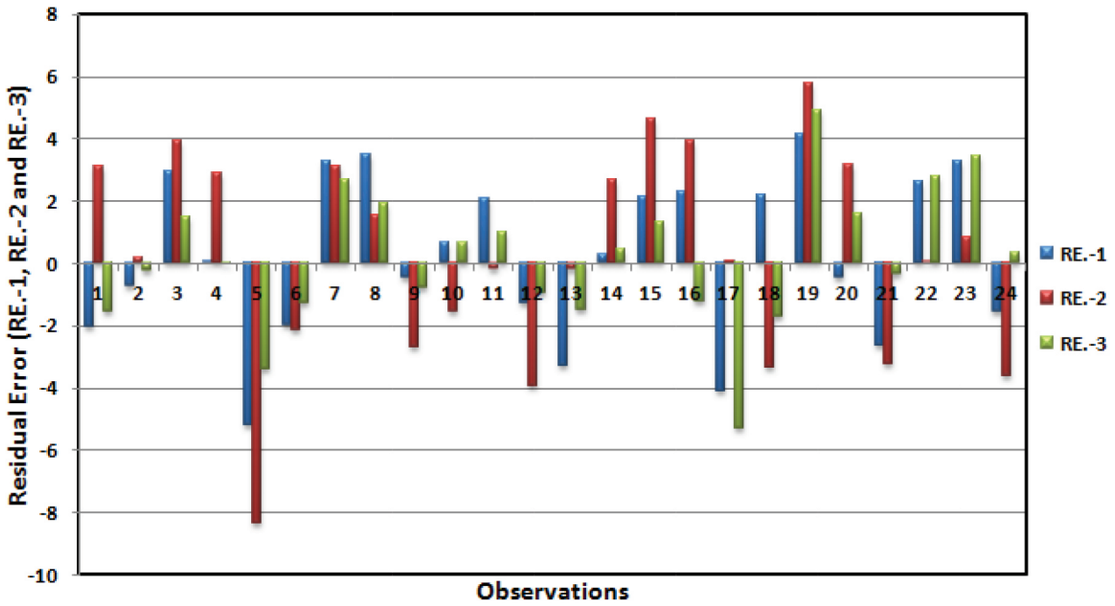

Fig. 8. The residual error (RE) between the average (Av. -1, Av. -2 and Av. -3) and the experimental inhibition efficiency of compounds 1–6 at different concentrations.

From the above results, the following conclusions can be drawn:

- The bis-benzimidazole derivatives namely: BBI, MBBI, EBBI, BBBI, HBBI and OBBI, present good inhibiting efficiencies *E*% of steel corrosion in acid medium at very low concentrations, and *E*% of these organic inhibitors can be directly linked to the structure electronic parameters.
- The AM1, HF and DFT calculations were used and DFT seems to be the most performed based on total energy and energy gap despite the highest CPU observed.
- The evolution of the undertaken global descriptors shows that ΔE, η, σ and ΔN follow the tendency of experimental inhibition efficiencies E_{exp}% of the studied inhibitors. In the opposite, E_{HOMO}, $E_{LUMO,}$ μ and χ seem not to be suitable to describe the E_{exp} % tendency.
- A direct correlation is established, for the different studied molecules, between the structure electronic properties and the corresponding corrosion inhibition efficiencies *E*% in acid medium by using three statistical models MLR, MPR and PLS.

Table 8
ANOVA for the three models (MLR, PLS and MPR)

Model	Source	SS	DF	MS	F_{obs}	F_{sta}	p-value
MLR	Regression	13181.36807	1	13181.36807	917.94398	4.30	<0.0001**
	Residual error	315.91263	22	13181.36807			
	Total	13497.2807	23				
PLS	Regression	13158.71175	1	13158.71175	855.04492	4.30	<0.0001**
	Residual error	338.56895	22	15.3895			
	Total	13497.2807	23				
MPR	Regression	13491.22354	1	13491.22354	49001.00515	4.30	<0.0001**
	Residual error	6.05716	22	0.27533			
	Total	13497.2807	23				

** Indicates highly significant at level 99%

– The higher values of the adjusted and the predicted determination coefficients (R^2_{adj}, R^2_{pred}) are considered as an irrefutable proof of the high predictive ability of these models. And MPR seems to be the most relevant model.
– Such study allows to rationalize, even to forecast the chemical reactivity, in order to predict the inhibiting efficiencies of new benzimidazole compounds, and to assist the organic chemist to the synthesis of promising molecules as corrosion inhibitors.

Acknowledgments

We are grateful to the ''Association Marocaine des Chimistes Théoriciens'' (AMCT) for the computation facilities.

Symbols

AM1	—	Austin Model 1
HF	—	Hartree-Fock
DFT	—	Density Functional Theory
B3LYP/6-311G	—	Becke, 3-parameter, Lee-Yang-Parr/ Basis set 6-311G
E_{HOMO}	—	Highest occupied molecular orbital energy
E_{LUMO}	—	Lowest unoccupied molecular orbital energy
μ	—	Dipole moment
V_i	—	Molecular critical volume
C_i	—	Concentration of inhibitor
Log P	—	Logarithm of the partition coefficient
M	—	Molar mass of the molecule
E_{cal} %	—	Calculated or predicted corrosion inhibition efficiency
E_{exp} %	—	Experimentally corrosion inhibition efficiency
QSPR	—	Quantitative Structure Property Relationships
MLR	—	Multiple Linear Regression
PLS	—	partial least squares
MPR	—	Multiple polynomial regression
N	—	Number of observations
r	—	Correlation coefficient
R^2	—	Determination coefficient
R^2_{adj}	—	Adjusted determination coefficient
R^2_{pred}	—	Predicted determination coefficient
PRESS	—	Predicted residual error sum of square
SS	—	Sum of squares
SS_{res}	—	Residual sum of squares
SS_{reg}	—	Regression sum of squares
SS_T	—	Total sum of squares
DF	—	Degree of freedom
MS	—	Mean of squares
F_{sta}	—	Statistic value of the Fisher.
F_{obs}	—	Observed value of the Fisher
p-Value	—	Probability value
α	—	Critical probability value
SD	—	Standard error (standard deviation)
N-1	—	Total degree of freedom
P	—	Explained degree of freedom
N-P-1	—	Residual degree of freedom

References

[1] H. El Sayed, A. El Nemr, S.A. Essawy, S. Ragab, Corrosion inhibitors Part V: QSAR of benzimidazole and 2-substituted derivatives as corrosion inhibitors by using the quantum chemical parameters, Progr. Org. Coat., 61 (2008) 11–20.
[2] E.S.H. El Ashry, A. El Nemr, S.A. Essawy, S. Ragab, Corrosion inhibitors-Part II: Quantum chemical studies on the corrosion inhibitions of steel in acidic medium by some triazole, oxadiazole and thiadiazole derivatives, Electrochim. Acta., 51 (2006) 3957–3968.
[3] E. Khamis, F. Bellucci, R.M. Latanision, E.S.H. El Ashry, Acid corrosion inhibition of nickel by 2-(triphenylphosphoranylidene) succinic anhydride, Corrosion, 47 (1991) 677–686.
[4] E. Khamis, E.S.H. El Ashry, A.K. Ibrahim, Synergistic action of vinyl triphenylphosphonium bromide with various anions on corrosion of steel, Br. Corros. J., 35 (2000) 150–154.
[5] A. Stoyanova, G. Petkova, S.D. Peyerimhoff, Correlation between the molecular structure and the corrosion inhibiting effect of some pyrophthalone compounds, Chem. Phys., 279 (2002) 1–6.
[6] M.A. Migahed, Electrochemical investigation of the corrosion behavior of mild steel in 2 M HCl solution in presence of 1-dodecyl-4-methoxy pyridinium bromide, Mater. Chem. Phys., 93 (2005) 48–53.
[7] A. Dadgarnezhad, I. Sheikhshoaie, F. Baghaei, Corrosion inhibitory effects of a new synthetic symmetrical Schiff-base on carbon steel in acid media, Anti-Corros. Methods Mater., 51 (2004) 266–271.
[8] G. Bereket, A. Pinarbasi, C. Ogretir, Benzimidazole-2-tione and benzoxazole-2-tione derivatives as corrosion inhibitors for aluminium in hydrochloric acid, Anti-Corros. Methods Mater., 51 (2004) 282–293.
[9] M.A. Quraishi, R. Sardar, Corrosion inhibition of mild steel in acid solutions by some aromatic oxadiazoles, Mater. Chem. Phys., 78 (2003) 425–431.
[10] H. Ashassi-Sorkhabi, B. Shaabani, D. Seifzadeh, Effect of some pyrimidine Schiff bases on the corrosion of mild steel in hydrochloric acid solution, Electrochim. Acta., 50 (2005) 3446–3452.
[11] H.L. Wang, H.B. Fan, J.S. Zheng, Corrosion inhibition of mild steel in hydrochloric acid solution by a mercapto-triazole compound, Mater. Chem. Phys., 77 (2003) 655–661.
[12] S. Martinez, I. Stagljar, Correlation between the molecular structure and the corrosion inhibition efficiency of chestnut tannin in acidic solutions, J. Molec. Struct. (Theochem), 640 (2003) 167–174.
[13] K.F. Khaled, K. Babic-Samardzija, N. Hackerman, Piperidines as corrosion inhibitors for iron in hydrochloric acid, J. Appl. Electrochem., 34 (2004) 697–704.
[14] I. Lukovits, A. Shaban, E. Kálmán, Thiosemicarbazides and thiosemicarbazones: Non-linear quantitative structure–efficiency model of corrosion inhibition, Electrochim. Acta., 50 (2005) 4128–4133.
[15] A. Lesar, I. Milošev, Density functional study of the corrosion inhibition properties of 1, 2, 4-triazole and its amino derivatives, Chem. Phys. Lett., 483 (2009) 198–203.
[16] E. Jamalizadeh, S.M.A. Hosseini, A.H. Jafari, Quantum chemical studies on corrosion inhibition of some lactones on mild steel in acid media, Corros. Sci., 51 (2009) 1428–1435.
[17] T. Arslan, F. Kandemirli, E.E. Ebenso, I. Love, H.M. Alemu, Quantum chemical studies on the corrosion inhibition of some sulphonamides on mild steel in acidic medium, Corros. Sci., 51 (2009) 35–47.
[18] I.B. Obot, N.O. Obi-Egbedi, Theoretical study of benzimidazole and its derivatives and their potential activity as corrosion inhibitors, Corros. Sci., 52 (2010) 657–660.

[19] M.K. Awad, M.R. Mustafa, M.M.A. Elnga, Computational simulation of the molecular structure of some triazoles as inhibitors for the corrosion of metal surface, Theochem., 959 (2010) 66–74.
[20] I. Ahamad, R. Prasad, M.A. Quraishi, Inhibition of mild steel corrosion in acid solution by Pheniramine drug: Experimental and theoretical study, Corros. Sci., 52 (2010) 3033–3041.
[21] P. Zhao, Q. Liang, Y. Li, Electrochemical, SEM/EDS and quantum chemical study of phthalocyanines as corrosion inhibitors for mild steel in 1mol/l HCl, Appl. Surf. Sci., 252 (2005) 1596–1607.
[22] F. Bentiss, M. Lebrini, M. Lagrenee, Thermodynamic characterization of metal dissolution and inhibitor adsorption processes in mild steel/2, 5-bis (n-thienyl)-1, 3, 4-thiadiazoles/hydrochloric acid system, Corros. Sci., 47 (2005) 2915–2931.
[23] J. Vosta, J. Eliasek, Study on corrosion inhibition from aspect of quantum chemistry, Corros. Sci., 11 (1971) 223–229.
[24] Z. El Adnani, M. Mcharfi, M. Sfaira, M. Benzakour, A.T. Benjelloun, M.E. Touhami, DFT study of 7-R-3methylquinoxalin-2 (1H)-ones (R= H; CH3; Cl) as corrosion inhibitors in hydrochloric acid, Int. J. Electrochem. Sci., 7 (2012) 6738–6751.
[25] O. Mokhtari, I. Hamdani, A. Chetouani, A. Lahrach, H. El Halouani, A. Aouniti, M. Berrabah, Inhibition of steel corrosion in 1M HCl by *Jatropha curcas* oil, J. Mater. Environ. Sci., 5 (2014) 310–319.
[26] S.S. Shivakumar, K.N. Mohana, Corrosion behavior and adsorption thermodynamics of some Schiff bases on mild steel corrosion in industrial water medium, Int. J. Corros., 2013 (2013), http://dx.doi.org/10.1155/2013/543204.
[27] Z. El Adnani, M. Mcharfi, M. Sfaira, M. Benzakour, A.T. Benjelloun, M. Ebn Touhami, DFT theoretical study of 7-R-3methylquinoxalin-2 (1H)-thiones (R= H; CH3; Cl) as corrosion inhibitors in hydrochloric acid, Corros. Sci., 68 (2013) 223–230.
[28] S.G. Zhang, W. Lei, M.Z. Xia, F.Y. Wang, Quantum chemical approach assisted by topological index, J. Molec. Struct. (Theochem), 732 (2005) 173–182.
[29] D. Glossman-Mitnik, CBS-QB3 calculation of quantum chemical molecular descriptors of isomeric thiadiazoles, J. Molec. Graphics Model., 25 (2006) 455–458.
[30] H. El Sayed, S.A. Senior, QSAR of lauric hydrazide and its salts as corrosion inhibitors by using the quantum chemical and topological descriptors, Corros. Sci., 53 (2011) 1025–1034.
[31] K.F. Khaled, Modeling corrosion inhibition of iron in acid medium by genetic function approximation method: A QSAR model, Corros. Sci., 53 (2011) 3457–3465.
[32] R. Todeschini, V. Consonni, A. Mauri, M. Pavan, Detecting "bad" regression models: Multi-criteria fitness functions in regression analysis, Anal. Chim. Acta., 515 (2004) 199–208.
[33] V. Consonni, D. Ballabio, R. Todeschini, Comments on the definition of the Q2 parameter for QSAR validation, J. Chem. Inf. Model., 49 (2009) 1669–1678.
[34] F.B. Growcock, Inhibition of steel corrosion in HCl by derivatives of cinnamaldehyde: Part I. Corrosion inhibition model, Corrosion, 45 (1989) 1003–1007.
[35] F.B. Growcock, W.W. Frenier, P.A. Andreozzi, Inhibition of steel corrosion in HCl by derivatives of cinnamaldehyde: Part II. Structure–activity correlations, Corrosion, 45 (1989) 1007–1015.
[36] P.G. Abdul-Ahad, S.H.F. Al-Madfai, Elucidation of corrosion inhibition mechanism by means of calculated electronic indexes, Corrosion, 45 (1989) 978–980.
[37] S. Cosnier, P. Dupin, D. Lavabre, A. Savignac, M. Comtat, A. Lattes, Electrocapillary study of the adsorption of 4-alkyl pyridine chlorides, Electrochim. Acta., 31 (1986) 1213–1218.
[38] I. Lucovits, K. Palfi, I. Bako, E. Kalman, LKP model of the inhibition mechanism of thiourea compounds, Corrosion, 53 (1997) 915–919.
[39] I. Lukovits, E. Kalman, G. Palinkas, Nonlinear group-contribution models of corrosion inhibition, Corrosion, 51 (1995) 201–205.
[40] I. Lukovits, I. Bakó, A. Shaban, E. Kálmán, Polynomial model of the inhibition mechanism of thiourea derivatives, Electrochim. Acta., 43 (1998) 131–136.
[41] F. Bentiss, M. Traisnel, H. Vezin, M. Lagrenée, Linear resistance model of the inhibition mechanism of steel in HCl by triazole and oxadiazole derivatives: Structure–activity correlations, Corros. Sci., 45 (2003) 371–380.
[42] M. Lebrini, M. Lagrenee, H. Vezin, L. Gengembre, F. Bentiss, Electrochemical and quantum chemical studies of new thiadiazole derivatives adsorption on mild steel in normal hydrochloric acid medium, Corros. Sci., 47 (2005) 485–505.
[43] Y. Abboud, B. Ihssane, B. Hammouti, A. Abourriche, S. Maoufoud, T. Saffaj, M. Berradaa, M. Charrouf, A. Bennamara, H. Hannache, Effect of some new diazole derivatives on the corrosion behavior of steel in 1M HCl, Desal. Water Treat., 20 (2010) 35–44.
[44] G. Gece, The use of quantum chemical methods in corrosion inhibitor studies, Corros. Sci., 50 (2008) 2981–2992.
[45] M. Bouayed, H. Rabaa, A. Srhiri, J.Y. Saillard, A. Ben Bachir, A. Le Beuze, Experimental and theoretical study of organic corrosion inhibitors on iron in acidic medium, Corros. Sci., 41 (1998) 501–517.
[46] H. Ma, S. Chen, Z. Liu, Y. Sun, Theoretical elucidation on the inhibition mechanism of pyridine–pyrazole compound: A Hartree Fock study, J. Mol. Struct. (Theochem), 774 (2006) 19–22.
[47] J.H. Henriquez-Roman, L. Padilla-Campos, M.A. Paez, J.H. Zagal, M.A. Rubio, C.M. Rangel, J. Costamagna, G. Cardenas-Jiron, The influence of aniline and its derivatives on the corrosion behavior of copper in acid solution: A theoretical approach, J. Mol. Struct. (Theochem), 757 (2005), 1–7.
[48] H. Ma, T. Song, H. Sun, X. Li, Experimental and theoretical elucidation on the inhibition mechanism of 1-methyl-5-mercapto-1, 2, 3, 4-tetrazole self-assembled films on corrosion of iron in 0.5M H_2SO_4 Solutions, Thin Solid Films, 516 (2008) 1020–1024.
[49] N. Boussalah, S. Ghalem, S. El Kadiri, B. Hammouti, R. Touzani, Theoretical study of the corrosion inhibition of some bipyrazolic derivatives: A conceptual DFT investigation Res. Chem. Interm., 38 (2012) 2009–2023.
[50] N.O. Obi-Egbedi, I.B. Obot, Inhibitive properties, thermodynamic and quantum chemical studies of alloxazine on mild steel corrosion in H2SO4, Corros. Sci., 53 (2011) 263–275.
[51] S.E. Nataraja, T.V. Venkatesha, H.C. Tandon, B.S. Shylesha, Quantum chemical and experimental characterization of the effect of ziprasidone on the corrosion inhibition of steel in acid media, Corros. Sci., 53 (2011) 4109–4117.
[52] K. Benbouya, B. Zerga, M. Sfaira, M. Taleb, M. Ebn Touhami, B. Hammouti, H. Benzeid, E.M. Essassi, WL, IE and EIS studies on the corrosion behavior of mild steel by 7-substituted 3-methylquinoxalin-2 (1H)-ones and thiones in hydrochloric acid medium, Int. J. Electrochem. Sci., 7 (2012) 6313–6330.
[53] C.C. Zhan, J.A. Nichols, D.A. Dixon, Ionization potential, electron affinity, electronegativity, hardness, and electron excitation energy: Molecular properties from density functional theory orbital energies, J. Phys. Chem. A., 107 (2003) 4184–4195.
[54] K.F. Khaled, Studies of iron corrosion inhibition using chemical, electrochemical and computer simulation techniques, Electrochim. Acta., 22 (2010) 6523–6532.
[55] V.S. Sastri, J.R. Perumareddi, Molecular orbital theoretical studies of some organic corrosion inhibitors, Corrosion, 53 (1997) 617–622.
[56] H. Abdi, Partial least square regression (PLS regression), Encyclopedia for Research Methods for the Social Sciences, 10 (2003) 792–795.
[57] M.J. Frisch, G.W. Trucks, H.B. Schlegel, G.E. Scuseria, M.A. Robb, J.R. Cheeseman, J.A. Montgomery Jr., T. Vreven, K.N. Kudin, J.C. Burant, J.M. Millam, S.S. Iyengar, J. Tomasi, V. Barone, B. Mennucci, M. Cossi, G. Scalmani, N. Rega, G.A. Petersson, H. Nakatsuji, M. Hada, M. Ehara, K. Toyota, R. Fukuda, J. Hasegawa, M. Ishida, T. Nakajima, Y. Honda, O. Kitao, H. Nakai, M. Klene, X. Li, J.E. Knox, H.P. Hratchian, J.B. Cross, C. Adamo, J. Jaramillo, R. Gomperts, R.E. Stratmann, O. Yazyev, A.J. Austin, R. Cammi, C. Pomelli, J.W. Ochterski, P.Y. Ayala, K. Morokuma, G.A. Voth, P. Salvador, J.J. Dannenberg, V.G.

Zakrzewski, S. Dapprich, A.D. Daniels, M.C. Strain, O. Farkas, D.K. Malick, A.D. Rabuck, K. Raghavachari, J.B. Foresman, J.V. Ortiz, Q. Cui, A.G. Baboul, S. Clifford, J. Cioslowski, B.B. Stefanov, G. Liu, A. Liashenko, P. Piskorz, I. Komaromi, R.L. Martin, D.J. Fox, T. Keith, M.A. Al-Laham, C.Y. Peng, A. Nanayakkara, M. Challacombe, P.M.W. Gill, B. Johnson, W. Chen, M.W. Wong, C. Gonzalez, J.A. Pople, 03, Revision B.01, Inc., Pittsburgh PA, (2003).

[58] G. Gece, S. Bilgiç, Quantum chemical study of some cyclic nitrogen compounds as corrosion inhibitors of steel in NaCl media, Corros. Sci., 51 (2009) 1876–1878.

[59] I.B. Obot, N.O. Obi-Egbedi, S.A. Umoren, Adsorption characteristics and corrosion inhibitive properties of clotrimazole for aluminium corrosion in hydrochloric acid, Int. J. Electr. Chem. Sci., 4 (2009) 863–877.

[60] N.O. Obi-Egbedi, I.B. Obot, M.I. El-Khaiary, S.A. Umoren, E.E. Ebenso, Computational simulation and statistical analysis on the relationship between corrosion inhibition efficiency and molecular structure of some phenanthroline derivatives on mild steel surface, Int. J. Electrochem. Sci., 6 (2011) 5649–5675.

[61] M.A. Quraishi, R. Sardar, Hector bases–a new class of heterocyclic corrosion inhibitors for mild steel in acid solutions, J. Appl. Electrochem., 33 (2003) 1163–1168.

[62] P. Hohenberg, W. Kohn, Inhomogeneous electron gas, Phys. Rev., 136 (1964) 864–871.

[63] I. Lukovits, E. Kalman, F. Zucchi, Corrosion inhibitors–correlation between electronic structure and efficiency, Corrosion, 57 (2001) 3–8.

[64] M. Jalali-Heravi, A. Kyani, Use of computer-assisted methods for the modeling of the retention time of a variety of volatile organic compounds: A PCA-MLR-ANN approach, J. Chem. Inf. Comput. Sci., 44 (2004) 1328–1335.

[65] J.M. Roque, T. Pandiyan, J. Crus, E. Garcia-Ochoa, DFT and electrochemical studies of tris (benzimidazole-2-ylmethyl) amine as an efficient corrosion inhibitor for carbon steel surface, Corros. Sci., 50 (2008) 614–624.

[66] Y. Abboud, A. Abourriche, T. Saffaj, M. Berrada, M. Charrouf, A. Bennamara, A. Cherqaoui, D. Takky, The inhibition of mild steel corrosion in acidic medium by 2, 2″-bis (benzimidazole), Appl. Surf. Sci., 252 (2006) 8178–8184.

[67] X. Wang, H. Yang, F. Wang, An investigation of benzimidazole derivative as corrosion inhibitor for mild steel in different concentration HCl solutions, Corros. Sci., 53 (2011) 113–121.

[68] F. Zhang, Y. Tang, Z. Cao, W. Jing, Z. Wu, Y. Chen, Performance and theoretical study on corrosion inhibition of 2-(4-pyridyl)-benzimidazole for mild steel in hydrochloric acid, Corros. Sci., 61 (2012) 1–9.

[69] Y. Tang, F. Zhang, S. Hu, Z. Cao, Z. Wu, W. Jing, Novel benzimidazole derivatives as corrosion inhibitors of mild steel in the acidic media. Part I: Gravimetric, electrochemical, SEM and XPS studies, Corros. Sci., 74 (2013) 271–282.

[70] A. Dutta, S.K. Saha, P. Banerjee, D. Sukul, Correlating electronic structure with corrosion inhibition potentiality of some bis-benzimidazole derivatives for mild steel in hydrochloric acid: Combined experimental and theoretical studies, Corros. Sci., 98 (2015) 541–550.

[71] J. Aljourani, K. Raeissi, M.A. Golozar, Benzimidazole and its derivatives as corrosion inhibitors for mild steel in 1M HCl solution, Corros. Sci., 51 (2009) 1836–1843.

[72] M. Mahdavian, S. Ashhari, Corrosion inhibition performance of 2-mercaptobenzimidazole and 2-mercaptobenzoxazole compounds for protection of mild steel in hydrochloric acid solution, Electrochim. Acta., 55 (2010) 1720–1724.

[73] X. Wang, Y. Wan, Y. Zeng, Y. Gu, Investigation of benzimidazole compound as a novel corrosion inhibitor for mild steel in hydrochloric acid solution, Int. J. Electrochem. Sci., 7 (2012) 2403–2415.